https://rbgeomorfologia.org.br/
ISSN 2236-5664

Revista Brasileira de Geomorfologia

v. 27, nº 2 (2026)

http://dx.doi.org/10.20502/rbg.v27i2.2707

Research Article

Soil Loss Estimation in Gullies of the Colônia Antônio Aleixo Basin, Manaus, Amazonas, Brazil

Estimativa de perda de solo em voçorocas da bacia Colônia Antônio Aleixo, Manaus, Amazonas, Brasil

Armando Brito da Frota Filho[1], Antonio Fábio Sabbá Guimarães Vieira[2], and Antonio Jose Teixeira Guerra[3]

[1] Universidade Federal do Amazonas, Departamento de Geografia, Manaus, Brazil. E-mail. armando.filho@ufam.edu.br ORCID: https://orcid.org/0000-0002-6133-7788

[2] Universidade Federal do Amazonas, Departamento de Geografia, Manaus, Brazil. E-mail. fabiovieira@ufam.edu.br ORCID: https://orcid.org/0000-0002-9416-8765

[3] Universidade Federal do Rio de Janeiro, Departamento de Geografia, Rio de Janeiro, Brazil. E-mail. antoniotguerra@gmail.com ORCID: https://orcid.org/0000-0003-2562-316X

Received: 20/06/2025; Accepted: 09/06/2026; Published: 23/06/2026

Abstract: Gullies in urban environments pose challenges to urban land-use planning due to their rapid development and the impact they cause on infrastructure and the physical environment. This study aimed at monitoring four gullies located in Colônia Antônio Aleixo watershed, in Manaus, Brazil, to analyze their morphometric characteristics and to estimate associated erosion rates. The study was based on cartographic records from 2006, 2012, and 2016, complemented by Unmanned Aerial Vehicle (UAV) surveys conducted in 2017 and 2020. The high-resolution imagery provided detailed information on the erosive features, while fieldwork supported data validation. The results indicate widening of the gullies and reduction in their depth, due to internal sediment deposition. Edge retreat also led to the coalescence of adjacent features. UAV monitoring made it possible to identify secondary landforms associated with reworking processes, such as headcut alcoves and small erosional channels. It is concluded that topographic profile analysis is an effective approach for understanding the morphology and evolutionary dynamics of gullies in urban environments.

Keywords: topographic profile; monitoring; watershed; UAV; erosion

Resumo: A ocorrência de voçorocas em áreas urbanas representa um desafio ao planejamento e à ocupação do solo, em função da intensidade com que esses processos evoluem e dos danos causados à infraestrutura e ao meio físico. Este estudo teve como objetivo monitorar quatro voçorocas localizadas na bacia hidrográfica Colônia Antônio Aleixo, em Manaus (AM), com a finalidade de analisar suas características morfométricas e estimar as taxas de erosão associadas. Para isso, utilizaram-se registros cartográficos dos anos de 2006, 2012 e 2016, complementados por levantamentos realizados com Veículo Aéreo Não Tripulado (VANT) em 2017 e 2020. As imagens geradas, com alta resolução espacial, permitiram detalhar as feições erosivas, enquanto os trabalhos de campo possibilitaram validar as informações obtidas. Os resultados indicam o alargamento das voçorocas e a redução de suas profundidades, sugerindo deposição interna de material. Também foi observada a coalescência de feições vizinhas, decorrente do recuo das bordas. O uso do VANT possibilitou identificar formas secundárias associadas ao retrabalhamento, como alcovas de regressão e caneluras. Conclui-se que a análise por perfis topográficos constitui uma ferramenta eficaz para compreender a morfologia e a dinâmica evolutiva de voçorocas em ambientes urbanos.

Palavras-chave: Perfil topográfico; monitoramento; bacia hidrográfica; VANT; erosão

1. Introduction

Monitoring gullies using high spatial resolution imagery constitutes a relevant approach for investigating erosional processes and their dynamics at both national and international scales. Such imagery may be acquired by satellites or Unmanned Aerial Vehicles (UAVs). Among the studies addressing this topic, those conducted by Shruthi et al. (2011) and Borrelli et al. (2022) stand out for employing high-resolution imagery for remote monitoring, including Ikonos satellite data. The integration of remotely sensed imagery with field surveys is essential, as in situ observations are fundamental for validating remotely acquired information and generating more accurate products that faithfully represent field conditions.

Studies conducted in South Africa by Krenz et al. (2018, 2019) and Krenz and Kuhn (2018) employed UAVs to generate Digital Terrain Models (DTMs), estimate areas susceptible to erosive processes, monitor erosion, quantify soil loss, and identify degraded areas with accuracy comparable to conventional field-based mapping. These authors emphasized that this approach enables the rapid and efficient identification of severely degraded areas while supporting assessments in heterogeneous landscapes. According to Krenz et al. (2018, 2019) and Krenz and Kuhn (2018), aerial surveys provide a broader landscape perspective than ground-based observations.

Loureiro (2019) and Loureiro et al. (2020) applied this technology to monitor and characterize a gully located along the RJ-155 highway between Angra dos Reis and Rio Claro, Brazil. Their results demonstrated that UAV-derived aerial imagery and derivative products enabled the identification of preferential runoff pathways and variations in sediment accumulation within the gully system.

In the Metropolitan Region of Manaus, UAV-generated imagery was first applied to gully characterization and monitoring by Silva (2017). The primary objective of that study was to evaluate the potential of this technology for monitoring gullies in remote and difficult-to-access areas of the Amazon. The author used UAV-derived products to describe, in detail, secondary erosional features such as headcut alcoves and potholes in gullies located in the Nova Cidade neighborhood and along the AM-010 and BR-174 highways. The results revealed that only the gullies located along the highways exhibited pedestals within their interiors, suggesting the influence of diffuse overland flow associated with splash erosion.

In Rio Preto da Eva, another municipality within the Metropolitan Region of Manaus, UAV monitoring was applied to three gullies. The survey considered morphometric parameters extracted from image processing and Digital Terrain Model generation, following the methodology proposed by Silva and Vieira (2020). The analysis enabled the identification of incision morphologies and their respective typologies based on the classification systems of Oliveira (1989) and Vieira (2008). Measurements of mean width, length, area (m^2), and eroded volume (m^3) were also obtained. The three incisions analyzed were responsible for more than 123,000 m^3 of eroded soil, rendering approximately 6,120 m^2 unusable and generating risk zones around two of the monitored features (Vieira et al., 2022).

In Iranduba, another municipality within the Metropolitan Region of Manaus, UAV monitoring was applied to six gullies over a one-year period to assess their morphological evolution (Silva, 2020). Among these features, one exhibited significant expansion in both area and volume, resulting in the loss of residential structures and urban infrastructure, including streets, drainage channels, and utility poles (Silva and Vieira, 2021).

These findings corroborate those reported by Santana (2019), who highlighted the growing application of UAVs in multiple fields, including environmental monitoring. UAVs have become established as relevant tools, particularly when integrated with specialized software for image processing and data generation. This integration enables more efficient exploration and analysis of difficult-to-access areas (Santana, 2019). This perspective is consistent with the discussion presented by Vieira and Frota Filho (2023) regarding the use of UAVs for monitoring erosional landforms and the need to integrate this technology with complementary techniques to improve analytical accuracy.

Within this context, detailed gully mapping is particularly important because it provides data on incision growth rates, eroded volumes, risk area identification, and off-site impacts. Accordingly, the present study aimed to characterize the evolution of four gullies in terms of morphometry and secondary erosional features through UAV-based monitoring and soil loss estimation.

2. Study Area

This study was conducted in the Colônia Antônio Aleixo watershed (Figure 1), located in the eastern sector of the urban area of Manaus, northern Brazil, with direct drainage into the Amazon River. Geologically, the study area is underlain by the Mesozoic Alter do Chão Formation (Franzinelli and Piucci, 1988). The local geomorphology belongs to the Eastern Amazon Plateau (Ross, 2000), which is characterized by intense erosional activity (Vieira, 2008).

Within the watershed, relief elevation does not exceed 120 m and is characterized by tabular interfluves that terminate in predominantly convex lower hillslopes (Vieira, 2008). The high density of erosional features is closely related to local geomorphological conditions, particularly slope gradient, the convex morphology of lower hillslope segments, and the stormwater drainage system (Vieira, 2008). The predominant soil classes are Oxisols, Ultisols, and Spodosols (Leal, 1996; Vieira, 1998, 2008; Barbosa, 2013; Frota Filho, 2016, 2021). For the gullies investigated in this study, incision development occurred predominantly in Oxisols.

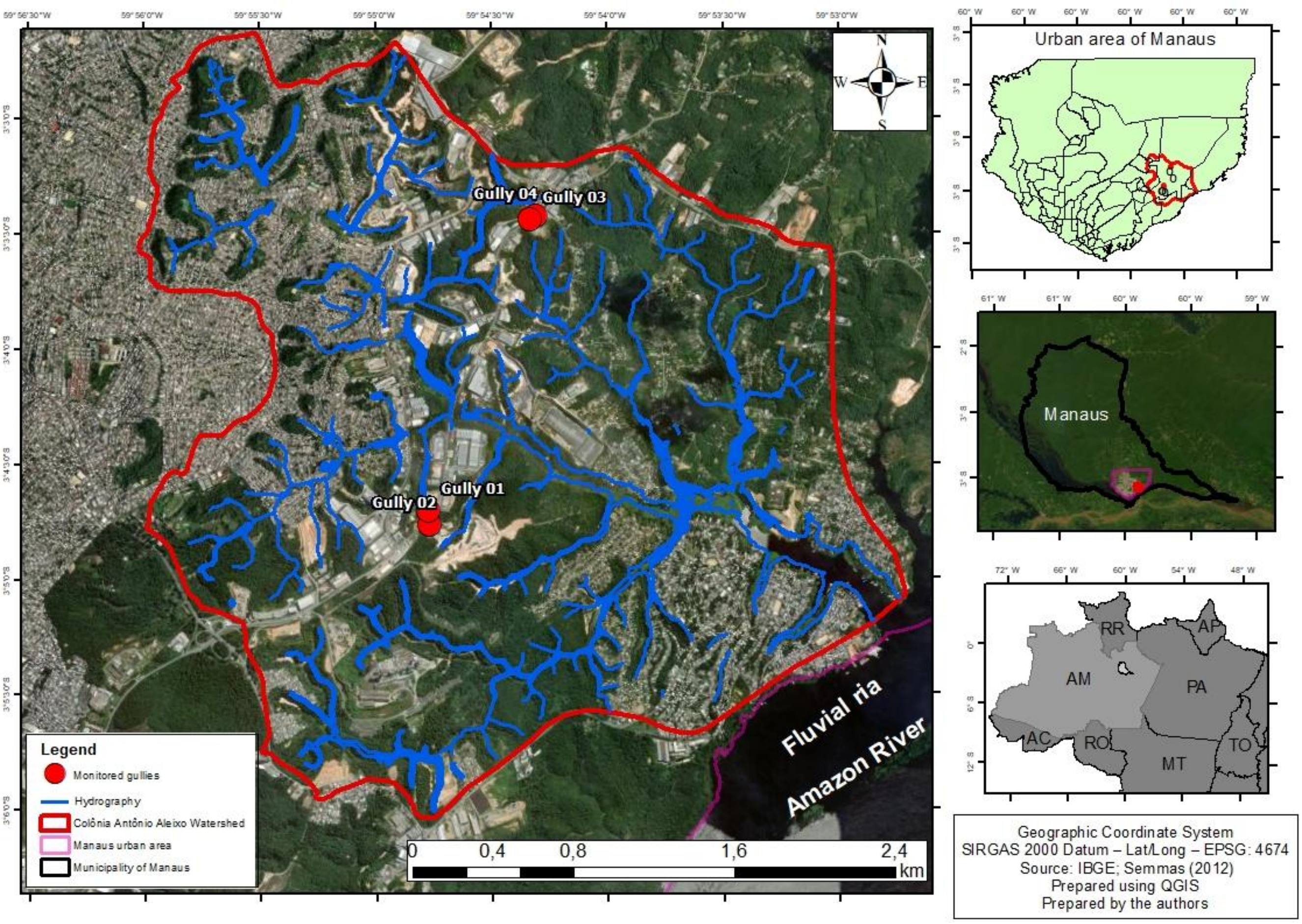

Figure 1. Location of the gullies monitored between 2017 and 2020 in the Colônia Antônio Aleixo watershed, Manaus, Amazonas, Brazil. Data sources: IBGE (2018) and ESRI. Prepared by the authors (2026) using ArcMap 10.8.

The regional climate is classified as humid equatorial, with a mean annual rainfall of 2,339.3 mm between 1986 and 2015 (D'Ávila Junior and Vieira, 2019). Mean annual air temperature during the same period was 27.9 °C, ranging from 23.7 °C to 32.1 °C, corresponding to the average minimum and maximum values, respectively (Santana, 2018). The hydrographic network is characterized by a dense dendritic drainage pattern (Frota Filho, 2016), with streams locally referred to as *igarapés*. The original vegetation cover is classified as Dense Ombrophilous Forest (Vieira, 1998).

The watershed contains the highest concentration of gullies within the urban area of Manaus, with 50 incisions recorded in 2008 (Vieira, 2008), 38 in 2012 (Frota Filho, 2012), 22 in 2016 (Frota Filho, 2016), and 26 in 2021 (Frota Filho, 2021). The reduction in the number of gullies over time is primarily associated with containment measures implemented by public authorities, along with interventions undertaken by local residents and civil society, such as infilling, which contributed to feature stabilization. Urbanization is identified as one of the main triggering factors of gully erosion within the watershed (Frota Filho, 2021).

3. Materials and methods

This study adopted a geomorphological monitoring approach that, according to Crozier et al. (2010), enables the quantitative and qualitative observation of landforms and landscape changes over time. Different techniques and instruments may be employed for this purpose, ranging from measuring tapes, compasses, and theodolites to satellite imagery and, more recently, data acquired by Unmanned Aerial Vehicles (UAVs).

The present investigation builds on the results of gully mapping and monitoring previously conducted in Manaus at three distinct periods: 2006, 2012, and 2021 (Vieira, 2008; Frota Filho, 2012, 2021). This study incorporates UAV-based monitoring into these previous datasets using an Unmanned Aerial Vehicle operated by the Laboratory for Sediment and Soil Analysis and Processing (LATOSSOLO/DEGEOG/UFAM). Field surveys were conducted to validate the results, specifically to confirm the location and morphometric characteristics of the monitored sites.

During the field campaigns, secondary erosional features associated with gully reworking processes were identified, including headcut alcoves, torrential potholes, and pedestals. Table 1 summarizes the location and morphometric characteristics of the hillslopes affected by the investigated gullies.

Table 1. Characteristics of the sites where the monitored gullies are located.

Gully	Coordinates	Hillslope gradient		Hillslope morphology
		(°)	(%)	
1	S 03° 4'41.85" O 59°54'46.45"	19.67°	31.91	Convex divergent
2	S 03° 4'46.28" O 59°54'49.13"	24.11°	39.79	Straight divergent
3	S 03° 3'25.64" O 59°54'19.78"	18.36°	26.66	Convex convergent
4	S 03° 3'24.66" O 59°54'18.20"	26.19°	43.62	Convex divergent

Source: Authors (2026).

Only four of the twenty-six gullies currently present within the Colônia Antônio Aleixo watershed were monitored in this study (Figure 1). These features are located in the Distrito Industrial II neighborhood and were selected because of their greater linear extent, depth, and volume, as well as their high activity and significant impacts on the urban drainage network. Site selection was based on field surveys, preliminary cartographic records, previous inventories and monitoring campaigns (Vieira, 2008; Frota Filho, 2016, 2021), and accessibility criteria.

Gully monitoring was conducted using a Phantom 4 Unmanned Aerial Vehicle (UAV) during survey flights performed on September 10, 2017, and January 7, 2020. Flight planning and execution were carried out using Pix4D software for the Phantom 4 platform (Figure 2).

The UAV was configured with 75% lateral and longitudinal overlap and equipped with a 4K-resolution camera tilted at 70°. Flight missions were planned in Grid Mission mode at an altitude of 60 m above ground level. This configuration provided a spatial resolution of 10 cm $pixel^{-1}$, with a planned Ground Sample Distance (GSD) of 2.79 cm $pixel^{-1}$, ensuring adequate coverage and high image quality.

According to Sousa (2018), the UAV system presented a total Root Mean Square Error (RMSE) of 9.81 m and a total Circular Map Accuracy Standard (CMAS) error of 21.04 m. Cartographic accuracy assessment indicated that the orthomosaic generated without ground control points exhibited geometric quality compatible with Class B Cartographic Accuracy Standard (PEC) products at a 1:10,000 scale and Class A products at a 1:25,000 scale, according to Sousa (2018). These parameters were adopted as reference values for assessing the reliability of the generated models and the subsequent morphometric analyses.

Figure 2. Unmanned Aerial Vehicle (UAV), DJI Phantom 4 model. Source: Prepared by the authors (2026). Photograph taken on February 5, 2024.

The images acquired during the UAV surveys were processed using Agisoft Metashape software based on the geometric altitude and GPS location data recorded for each photograph. From these data, a dense point cloud was generated, followed by model texturing. In the subsequent processing stage, the Digital Terrain Model (DTM), orthomosaics, and three-dimensional models were generated. These products were then analyzed in a Geographic Information System (GIS) environment using QGIS software.

Based on the processing performed in this environment, derivative products, including the Digital Terrain Model (DTM), contour lines, and orthophotos, were generated (Figure 3), providing the basis for gully delineation. Delineation was performed manually from the initial boundaries of the erosional features, resulting in shapefile (.shp) polygon files representing each individual incision.

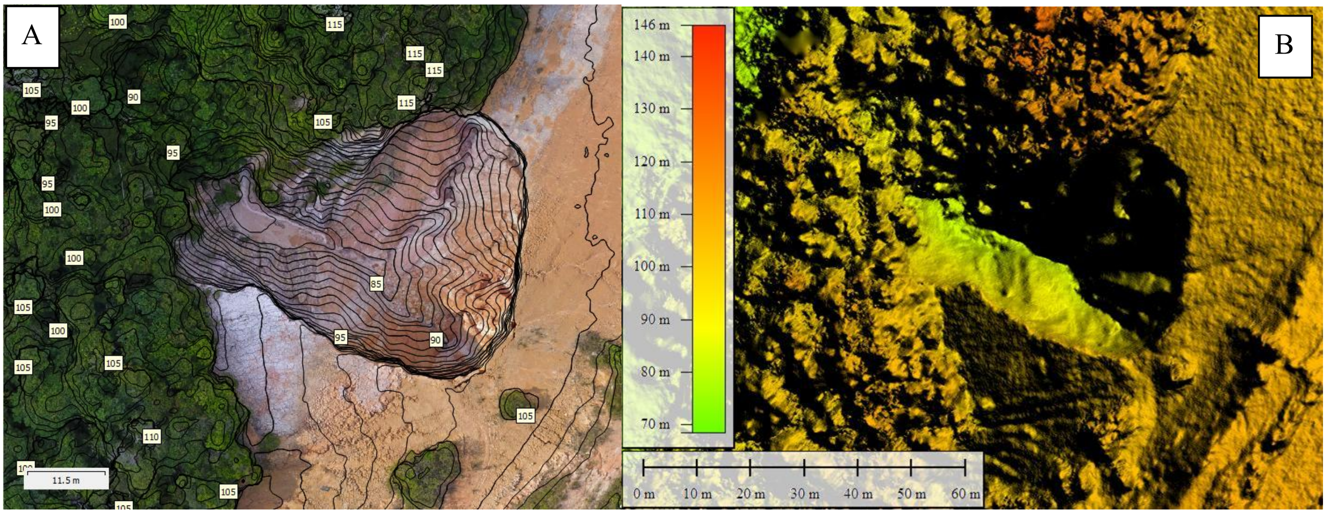

Figure 3. Delimitation of gully 1 (A) and the Digital Terrain Model (DTM) (B), generated from contour lines (A). Prepared by the authors (2026).

The adopted methodology included the application of digital aerial photogrammetry based on the Structure from Motion–Multi View Stereo (SfM-MVS) principle, a technique that enables the generation of three-dimensional models from overlapping images acquired at different viewing angles. This method allows the reconstruction of dense point clouds and high-resolution surface models, even in the absence of ground control points. In UAV-based studies, this approach has demonstrated high efficiency for terrain modeling and morphometric analysis of erosional landforms, particularly in difficult-to-access areas (Bitencourt et al., 2021).

Subsequently, morphometric parameters were calculated, including length, mean width, mean depth, area, and volume, in addition to the generation of transverse and longitudinal incision profiles within the GIS environment. Based on the imagery processed in Agisoft Metashape, length, mean width, and mean depth were obtained, enabling the calculation of eroded area (length × width), eroded volume (area × depth), and soil loss (volume × soil bulk density).

Repeated monitoring surveys made it possible to quantify changes in eroded area and volume between the analyzed periods, expressed in m² and m³, respectively. The surveys also enabled the assessment of feature expansion or reduction over the monitored years and the estimation of annual linear expansion rates (m year⁻¹) for each incision.

In addition, morphological changes in the gullies were assessed according to "Type," following the classification proposed by Oliveira (1989) (Figure 4); "Shape," according to Vieira (2008) (Figure 5); and size classes, based on the classification system proposed by Vieira and Albuquerque (2004) (Table 2).

Table 2. Gully size classification according to eroded volume (m³).

Class	Eroded volume (m³)	Size category
01	Up to 999 m³	Very small
02	De 1,000 m³ - 9,999 m³	Small
03	Entre 10,000 - 19,999 m³	Medium
04	Entre 20,000 - 40,000 m³	Large
05	> 40,000 m³	Very large

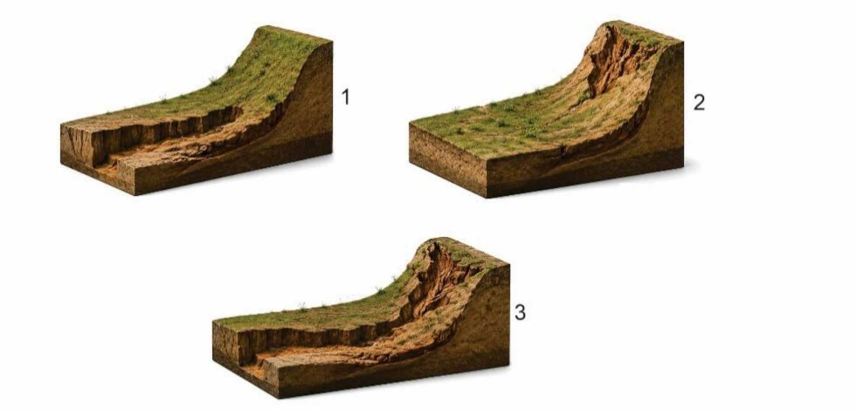

Figure 4. Types of gullies: Type 1 - connected gully; Type 2 - disconnected gully; Type 3 - integration of both types of gullies. Source: Oliveira (1989).

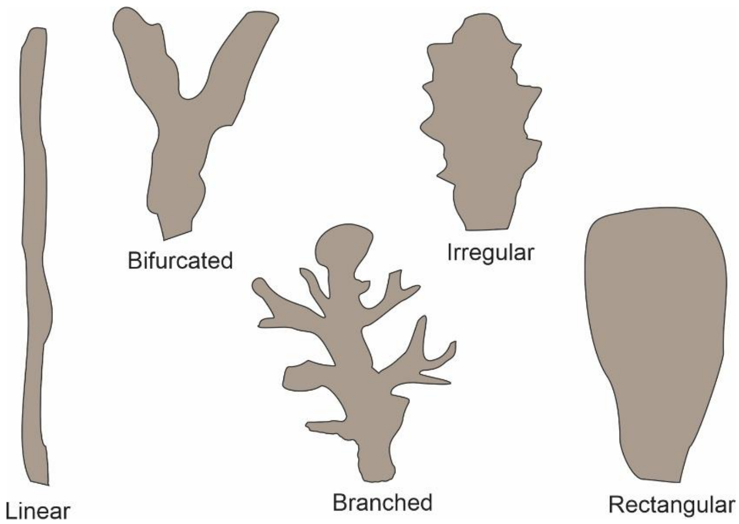

Figure 5. Gully morphologies (Vieira, 2008).

4. Results

The intensification of hydrogeomorphological dynamics was further enhanced by urbanization processes within the study area. Accordingly, monitoring surveys sought to characterize gully evolution in terms of morphometry and secondary erosional features, as well as to estimate soil loss from the investigated incisions, thereby enabling the determination of the size class of these erosional landforms.

3.1. Incision morphometry: growth rates and expansion patterns

The monitoring surveys conducted in 2017 and 2020 (Figure 6) enabled the analysis of the morphology and expansion of Gully 01. Examination of the transverse profiles (AB, CD, and EF) revealed a U-shaped morphology, which is characteristic of this type of erosional feature (Figure 6).

From a morphological perspective, the evolution of profile AB between 2017 and 2020 exhibited the greatest lateral expansion. This behavior may be attributed to the large contributing area associated with runoff concentration, combined with the presence of highly friable soil material. It should be noted that soil analysis was not the primary objective of this study but was derived from complementary research conducted in the same area (Frota Filho, 2021). In that investigation, the soil was classified as sandy loam, comprising 71.03% sand, 22.46% silt, and 6.51% clay. These textural properties contributed to the higher erodibility of the material.

Between 2017 and 2020, changes in the internal configuration of the incision were identified through the analysis of Digital Terrain Models and aerial imagery. Sediment redistribution between the monitoring periods was evidenced by variations in contour line configuration throughout the analyzed interval (Figure 7).

The integrated analysis of the figures and the geoprocessed morphometric data allowed the quantification of the changes that occurred between the monitoring campaigns, identifying a 0.03 m reduction in gully depth. This decrease resulted from the accumulation of alluvial-colluvial sediments within the incision (Table 3). The longitudinal profile exhibited an expansion of 2.24 m during this period. Among the transverse profiles analyzed, profile AB recorded the greatest increase, with an expansion of 2.23 m, whereas profile CD exhibited a more limited expansion of 0.20 m.

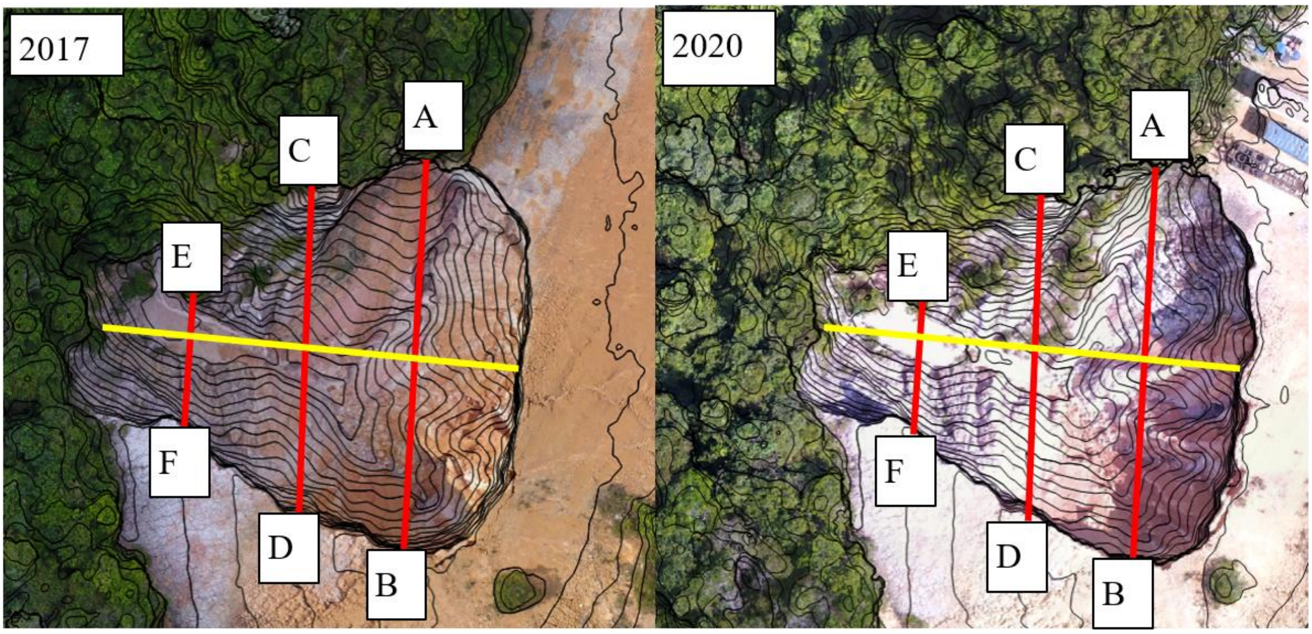

Figure 6. Gully 01 during the 2017 and 2020 monitoring surveys, showing orthorectified imagery, 5-m contour intervals, a scale of 1:1,000, cross-sectional profiles (AB, CD, and EF, in red), and the longitudinal profile (in yellow). Source: Authors (2026).

Table 3. Summary of morphometric parameters analyzed during the monitoring surveys of Gully 01.

Gully 01			
Parameter	**2017**	**2020**	**Changes**
Cross-section profile AB (m)	39.75	41.98	+2.23*
Cross-section profile CD (m)	32.74	32.94	+0.20*
Cross-section profile EF (m)	24.42	24.81	+0.39*
Mean Cross-section profile (m)	32.30	33.24	+0.94*
Longitudinal profile (m)	52.19	54.42	+2.24*
Depth (m)	21.92	21.89	-0.03**
Area (m^2)	1 685.85	1 809.06	+123.21*
Volume (m^3)	36 960.60	39 596.77	+2 636.16*

*Increase between monitoring periods. **Decrease between monitoring periods. Source: Authors (2026).

The longitudinal profile exhibited changes between the monitoring periods, with sediment accumulation observed in the downstream sector of the incision in 2020. This interpretation is corroborated by transverse profile EF, which clearly shows the deposition of these sediments. This process also explains the reduction in gully depth, likely associated with erosion of margin F and the subsequent deposition of sediment at the base of the incision.

Transverse profile AB exhibited the highest lateral growth rate, with an expansion of 2.23 m. An increase in depth was also observed in this sector. In contrast, profile CD remained relatively stable in terms of width, exhibiting an increase of only 0.20 m, accompanied by a slight increase in depth.

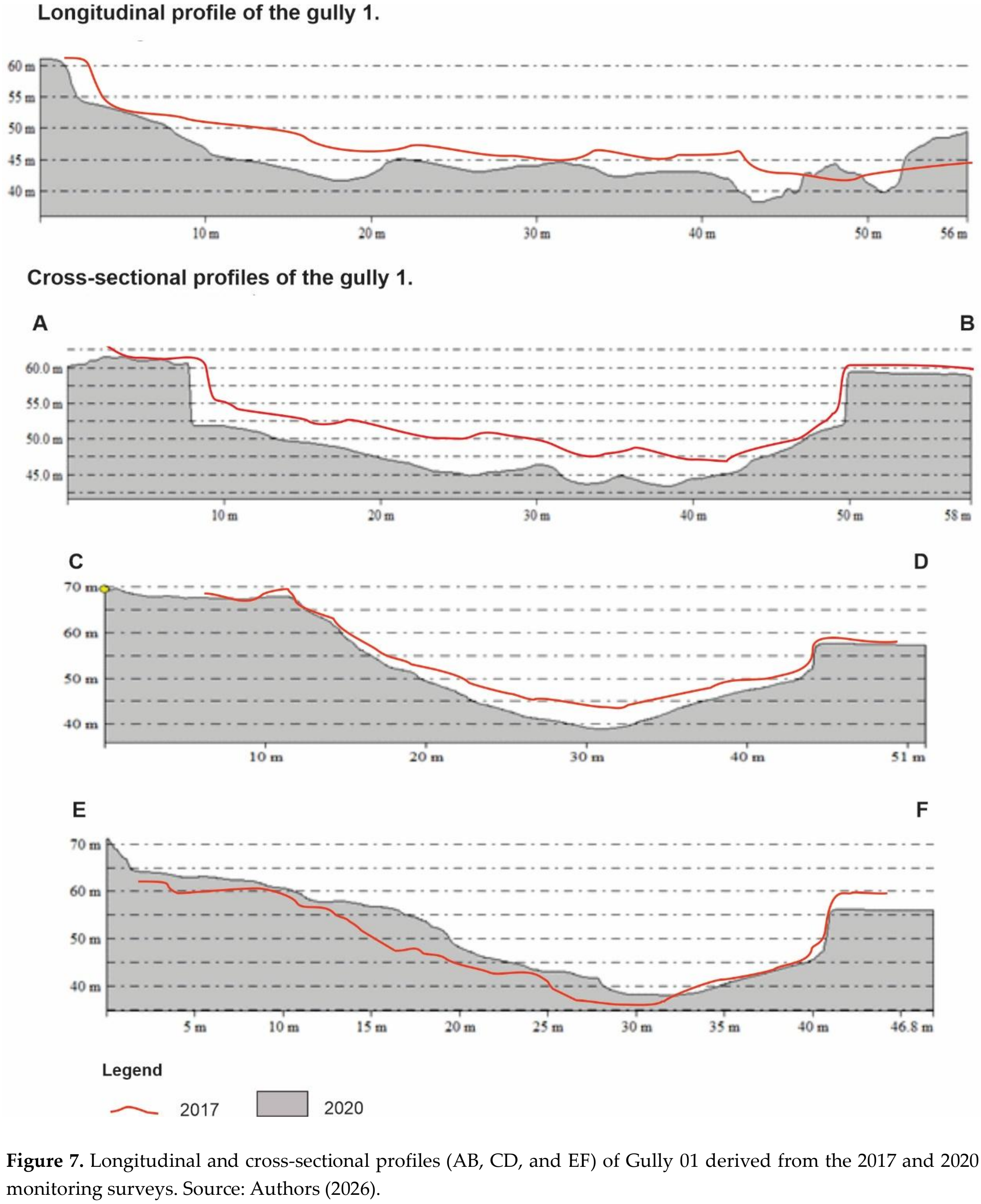

Figure 7. Longitudinal and cross-sectional profiles (AB, CD, and EF) of Gully 01 derived from the 2017 and 2020 monitoring surveys. Source: Authors (2026).

Gully 02 remained classified as connected to the hydrographic network and retained a linear morphology (Figure 8). The eroded volume was estimated at 42,173.50 m³, classifying this incision as very large. Table 4 summarizes the monitoring data, highlighting gully expansion in both width and length. These changes were further confirmed by the transverse profiles presented in Figure 9.

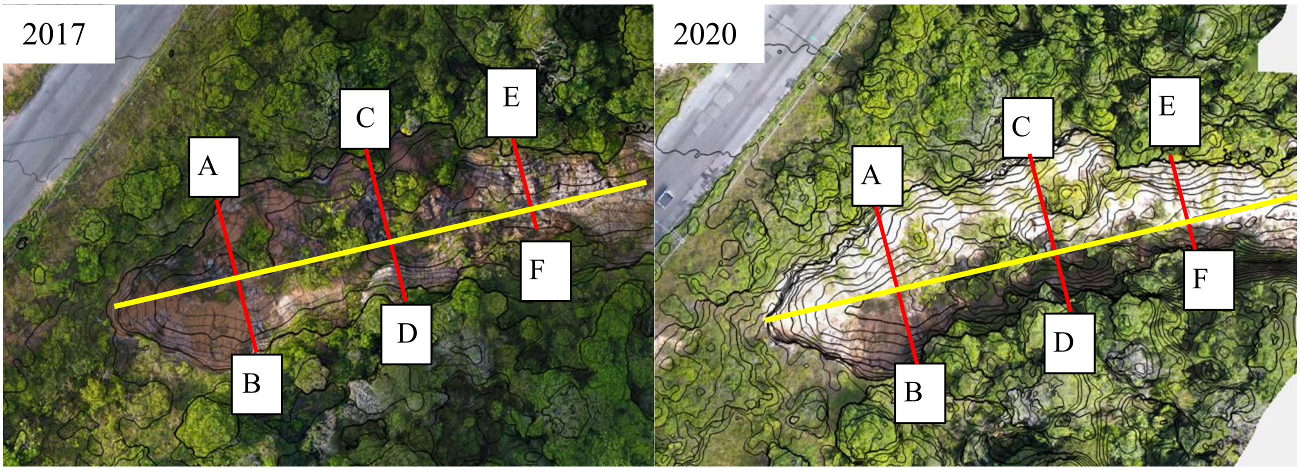

Figure 8. Gully 02 during the 2017 and 2020 monitoring surveys, showing orthorectified imagery, 5-m contour intervals, a scale of 1:1,000, transverse profile traces (AB, CD, and EF, in red), and the longitudinal profile (in yellow). Source: Authors (2026).

Table 4. Summary of the parameters analyzed during the monitoring of gully 02.

Gully 02			
Parameter	**2017**	**2020**	**Changes**
Cross-section profile AB (m)	23.38	22.49	+0.10*
Cross-section profile CD (m)	21.73	21.92	+0.18*
Cross-section profile EF (m)	21.62	24.24	+2.62*
Mean Cross-section profile (m)	**22.24**	**22.88**	**+0.64***
Longitudinal profile (m)	84.04	84.59	+0.54*
Depth (m)	21.89	26.79	+4.90*
Area (m^2)	**1 869.44**	**1 926.87**	**+57.44***
Volume (m^3)	**40 921.95**	**51 622.89**	**+10 700.94**

*Increase between monitoring periods. **Decrease between monitoring periods. Source: Authors (2026).

Among the analyzed profiles, profile EF exhibited the greatest morphological evolution, with an expansion of 2.62 m between 2017 and 2020. This behavior indicates greater erosive activity in this sector of the incision (Figure 9), where erosional processes promote the formation of rills that contribute to margin collapse, with possible block failure along the gully walls. This process may explain the increase in width observed in this sector (Figure 9, profile EF).

The observed dynamics also contributed to incision deepening, which reached 4.90 m, increasing the eroded volume from 40,921.95 m^3 in 2017 to 51,622.89 m^3 in 2020 (Table 4). This behavior is associated with the removal of material previously deposited within the gully, as evidenced by the evolution of the longitudinal and transverse profiles.

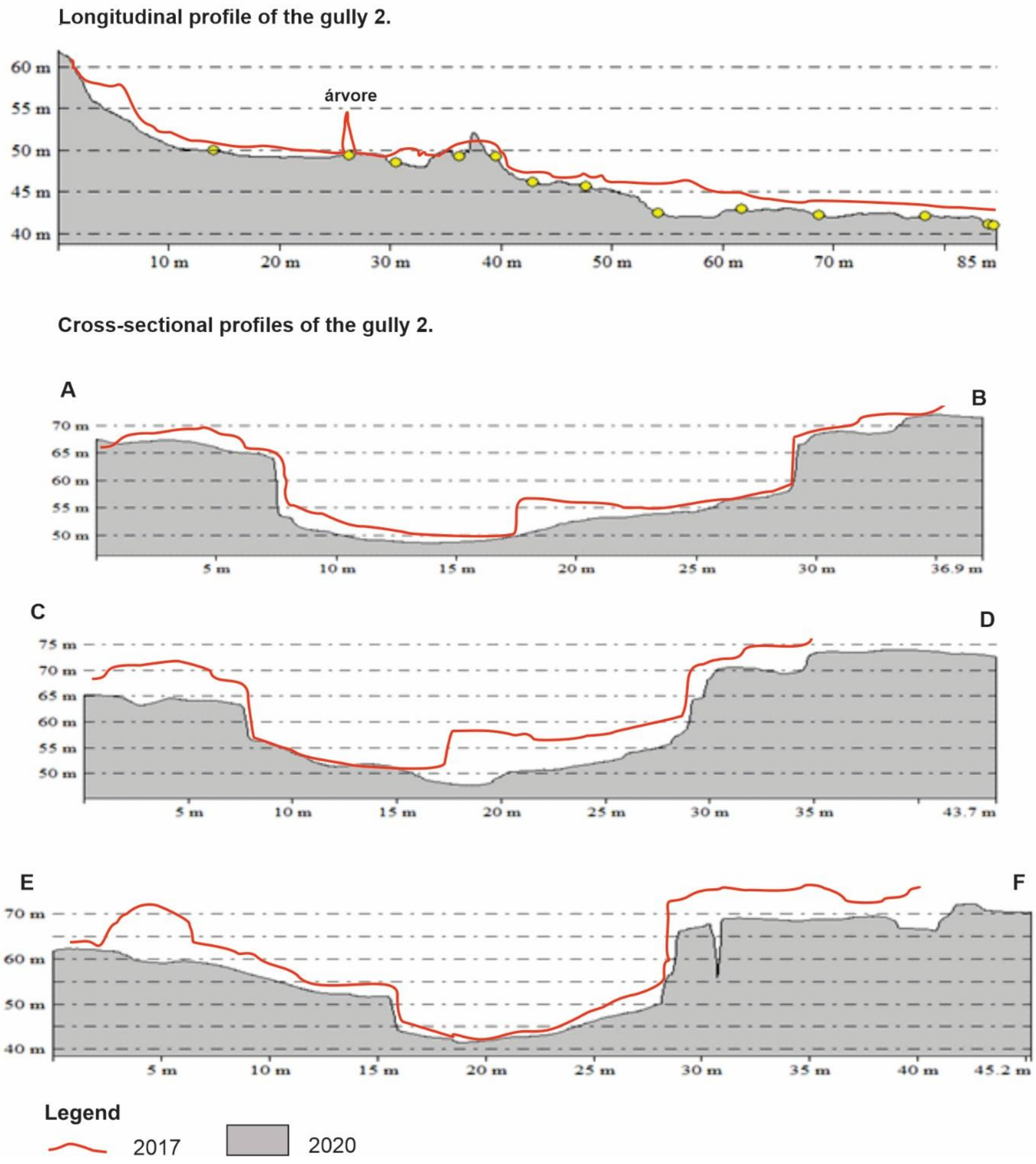

Figure 9. Longitudinal and cross-section profiles (AB, CD, and EF) of Gully 02 for the years 2017 and 2020. Source: Authors (2026).

Limited growth was observed in cross-section profiles AB and CD, with expansions of 0.10 m and 0.18 m, respectively, when compared to profile EF, which exhibited an expansion of 2.62 m (Table 4). This behavior indicates a reduction in the contributing area because of longitudinal headward progression toward the interfluve, thereby decreasing the concentrated flows responsible for sediment transport. Consequently, transport capacity decreases, due to slope reduction and the associated decline in kinetic energy and entrainment potential.

As the incision advances toward the interfluve, the contributing area is progressively reduced. This results in a proportional decrease in concentrated flow discharge, directly affecting kinetic energy and erosive potential, which in turn reduces the linear expansion rate of the gully, a process characterized by headward retreat. Therefore, as the headcut of this erosional feature progresses toward the interfluve, lower water accumulation is directed into the incision, favoring progressive stabilization.

This relative stability enabled vegetation establishment within the gully interior (Figure 6), a pattern also reflected in the growth dynamics recorded in cross-section profiles AB and CD (Figure 9). Comparison between the longitudinal profiles from the two monitoring periods (Figure 9) reveals a reduction in the volume of material deposited within the incision. The Digital Elevation Model corresponding to 2020 shows a more irregular basal surface near the headcut, compared with the previous monitoring period, an interpretation corroborated by the deeper-cross-section profiles.

Regarding Gullies 03 and 04, this hillslope initially exhibited a system composed of four gullies (Figure 10), which subsequently underwent evolutionary and capture processes, resulting in the elimination of one feature due to coalescence between Gullies 04 and 05.

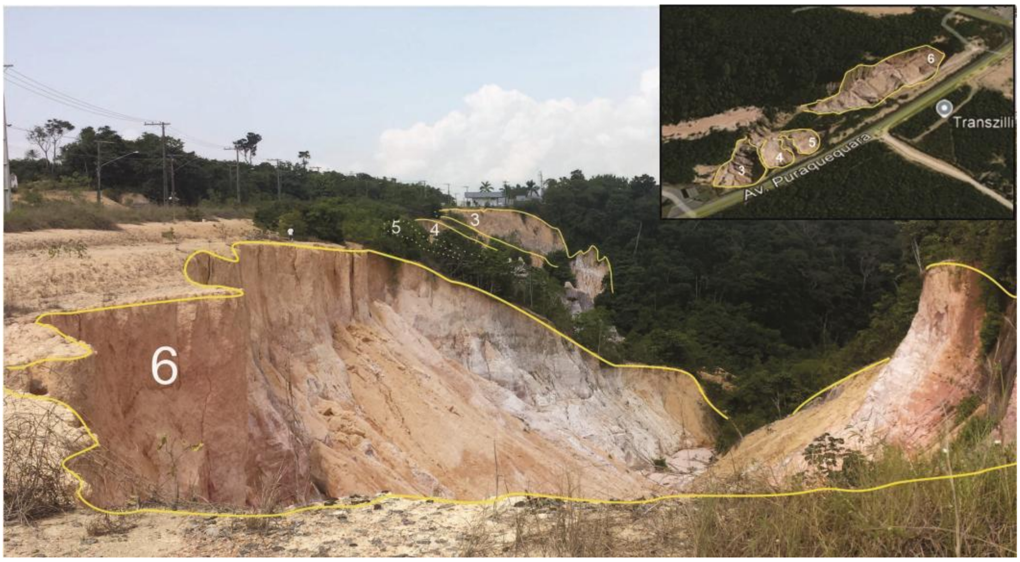

Figure 10. Evolution of gullies in the Distrito Industrial II neighborhood, Colônia Antônio Aleixo watershed. Sources: Authors (2013) and © Google Earth (2005). Prepared by the authors (2026).

In addition to these features, Gully 06 deserves particular attention, although it was not included in this monitoring campaign, due to morphological changes associated with the loss of characteristic gully features, such as a flat basal floor and vertical walls, giving way to terrace formation within its interior.

Within this context, Gullies 03 and 04, which constitute the focus of this study, exhibit similar morphological characteristics and were classified as **integrated**, **rectangular**, and **very large** (Figure 11).

Gully 03 exhibited increases in both length and width, whereas Gully 04 showed reductions in area and volume (Table 5). This decrease resulted from the collapse of a portion of the incision wall, causing the partial loss of morphological characteristics typically associated with gullies, particularly vertical walls. Consequently, a reduction in length was observed, directly affecting eroded areas and volume. This behavior is related to the fact that the incisions on this hillslope share the same erosional source, represented by concentrated stormwater runoff conveyed through drainage channels, which has favored their progressive integration over time.

About Gully 03, cross-section profiles AB and CD showed clear evolution, with expansions of 2.62 m and 3.74 m, respectively. Profile EF exhibited the greatest lateral development, with an increase of 10.9 m during the monitoring period between 2017 and 2020, accompanied by downstream sector leveling, as suggested by the imagery presented in Figure 8. This behavior indicates intensified erosive activity in this sector of the incision (Figures 12 and 13), associated with the erosion of vertical walls.

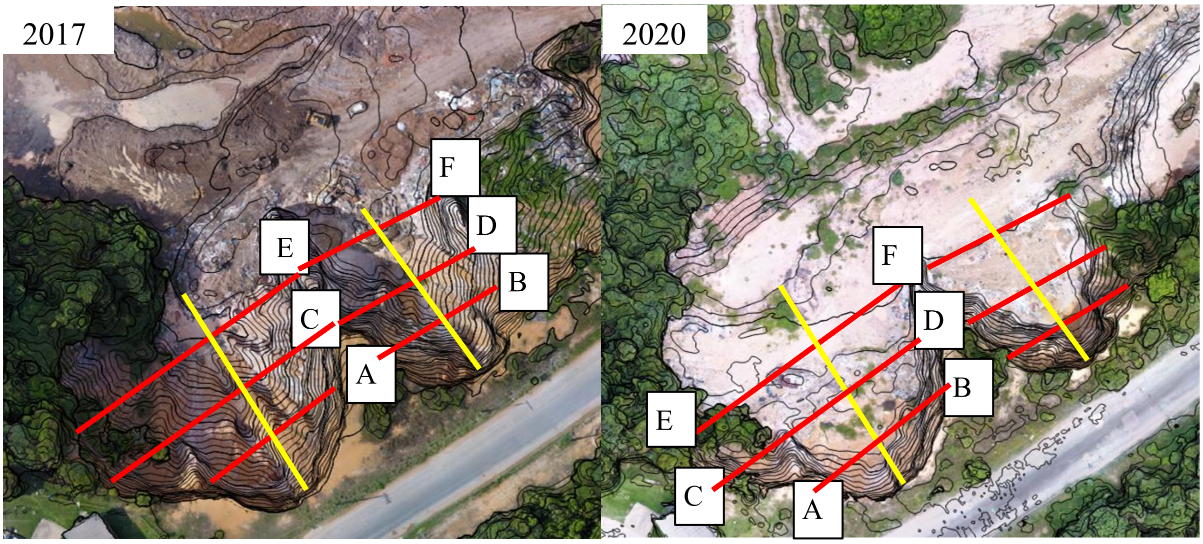

Figure 11. Gullies 03 and 04 during the 2017 and 2020 monitoring surveys, showing orthorectified imagery, 5-m contour intervals, a scale of 1:1,000, cross-sectional profiles (AB, CD, and EF, in red), and the longitudinal profile (in yellow). Source: Authors (2026).

Table 5. Summary of the parameters analyzed during the monitoring of gullies 03 and 04.

Parameter	**Gully 03**			**Gully 04**		
Cross-section profile AB (m)	**2017**	**2020**	**Changes**	**2017**	**2020**	**Changes**
Cross-section profile CD (m)	54,13	56,75	+2,62*	31,57	33,60	+2,03*
Cross-section profile EF (m)	53,01	56,75	+3,74*	33,59	34,50	+0,91*
Mean Cross-section profi (m)	44,92	55,81	+10,90*	30,53	0,00***	-30,53**
Longitudinal profile (m)	50,69	56,44	+5,75*	31,90	22,70	-9,20**
Depth (m)	61,61	61,72	+0,11*	47,63	33,40	-14,23**
Area (m²)	34,69	26,62	-8,07**	32,80	25,77	-7,03**
Volume (m³)	**3 122,67**	**3 483,38**	**360,71***	**1 519,32**	**758,20**	**-761,12****
Transverse profile AB (m)	**108 322,39**	**92 713,75**	**-15 608,65****	**49 833,64**	**19 536,60**	**-30 297,04****

*Increase between monitoring periods. **Decrease between monitoring periods. Source: Authors (2026).

The same pattern of intensified erosive activity was observed in profiles AB and CD with respect to depth, resulting in incision flattening, as suggested by classical concepts associated with flat-bottomed gully morphology. Because of this process, sediment deposition occurred within the incision, contributing to depth reduction and reflecting a decrease in eroded volume between monitoring periods. Comparison of the profiles from the analyzed years indicates an accumulation exceeding 5 m of deposited material (Figure 12).

From a longitudinal perspective, virtually no growth was observed during the monitoring period, corresponding to only 0.11 m. As observed for Gully 02, this feature exhibits a reduced contributing area, as it is located close to the interfluve and its primary source of concentrated flow corresponds to wastewater discharge originating on the upslope along the access road.

The cross-section profiles reveal lateral expansion and incision deepening. However, the longitudinal profile shows sediment accumulation in specific sectors (Figure 10), resulting in a reduction in eroded volume between 2017 and 2020, from 108,322.39 m³ to 92,713.75 m³. Accordingly, sediment retention within the incision is estimated at 15,608.65 m³ (Table 5).

It is noteworthy that the contributing area remained practically unchanged, considering that longitudinal gully growth advanced only 0.11 m toward the interfluve. The proximity between the gully headcut and the interfluve indicates a limited contributing area for generating concentrated flows directed into the incision, suggesting relative stability of this feature in this sector. In contrast to the headcut sector, lateral expansion was more pronounced in transverse profiles AB, CD, and EF, with expansions of 2.62 m, 3.74 m, and 10.9 m, respectively, as shown in Table 5 and Figure 12.

The integrated analysis of longitudinal and cross-section profile evolution reveals internal sediment redistribution within the gully, as evidenced by depth reduction in sectors AB, CD, and EF, with the latter being affected to a lesser extent. In the central portion of the longitudinal axis, sediment accumulation formed a deposit approximately 5 m thick (Figure 12, longitudinal profile).

Regarding incision area, an increase from 3,122.67 m² to 3,483.38 m² was observed, corresponding to an expansion of 360.71 m². Part of the material eroded from the gully walls remained partially deposited within the incision, causing a reduction in depth and, consequently, a decrease in eroded volume within the central sector of the longitudinal axis (Figure 12, longitudinal profile; Table 5).

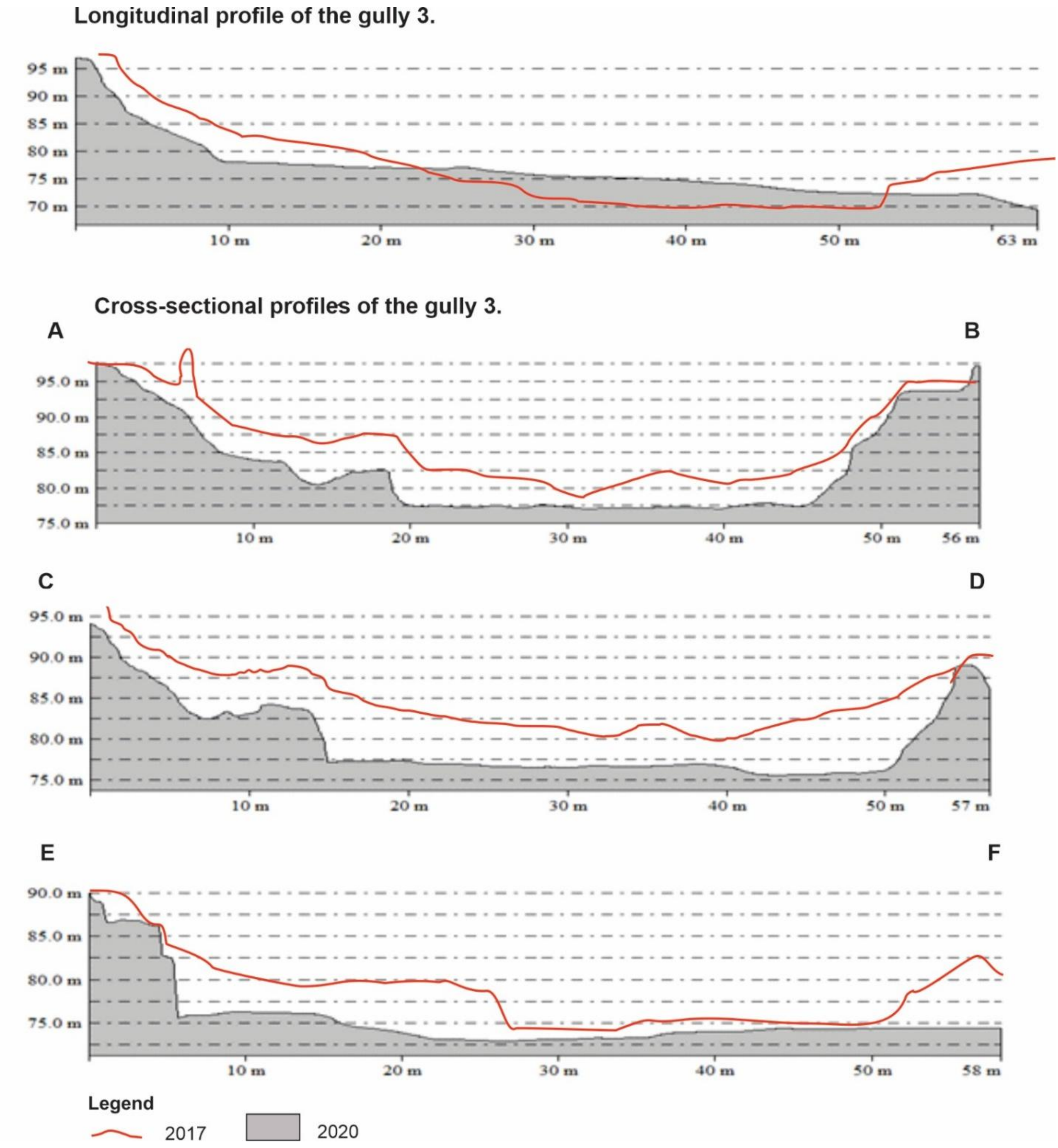

Figure 12. Longitudinal and transverse profiles (AB, CD, and EF) of gully 03, obtained during the 2017 and 2020 monitoring campaigns. Source: Prepared by the authors (2026).

Gully 04 (Figure 13) showed a reduction in area and volume due to the collapse of the incision walls in its final section (Figure 11, transverse profile EF), as presented in Table 5. This change resulted in a decrease in feature length from 47.63 m to 33.40 m, directly affecting area values, which decreased from 1,519.32 m² to 758.20 m², and volume, which was reduced from 49,833.64 m³ to 19,536.6 m³.

On the other hand, transverse profiles AB and CD recorded width increases of 2.03 m and 0.91 m, respectively. The internal dynamics of the erosive feature proved to be intense, with significant removal of the alluvial-colluvial deposits present within it (Figures 11 and 13), resulting in increased depth. The material observed in profiles AB and CD was transported downstream (Figure 11, longitudinal profile).

Figure 13. Longitudinal and cross-sectional profiles (AB, CD, and EF) of Gully 04 derived from the 2017 and 2020 monitoring surveys. Source: Authors (2026).

Based on the data derived from UAV-processed imagery, it was possible to calculate the growth rates of the four monitored incisions in terms of area and volume. Considering only days with recorded precipitation, Gully 03 exhibited the highest surface growth rate, reaching 0.79 m^2 day^{-1} (Table 6). This result indicates the high erodibility of soils in the study area, as evidenced by the increase in width observed in the cross-section profiles, although, as discussed in the previously analyzed profiles, part of the mobilized sediment was deposited within the incision.

Table 6. Surface growth rates of the investigated gullies (m^2 day^{-1}).

Gully.	Area (m^2) 2017 (A)	Area (m^2) 2020 (B)	Difference (B – A = C) (m^2)	Cumulative precipitation 2017–2020 (mm)	Surface growth rate (m^2 day^{-1}) Total period (850 days)*	Surface growth rate (m^2 day^{-1}) Rainfall days only (453 days)**
1	1685,85	1809,06	123,21	5839,1	0,14	0,27
2	1869,44	1926,87	57,44	5839,1	0,06	0,12
3	3122,67	3483,38	360,71	5839,1	0,42	0,79
4	1519,32	758,20	-761,12	5839,1	***	***

* Total monitoring period (850 days). ** Days with recorded precipitation (453 days).

*** Rate not calculated due to negative surface variation. *Source: Authors (2026).*

However, due to the occurrence of negative volumetric growth associated with sediment deposition on the incision floor, it was not possible to determine volumetric growth rates for Gullies 03 and 04. Similarly, the surface growth rate of Gully 04 could not be estimated, since wall collapse in its terminal section compromised analytical accuracy.

Accordingly, Gully 02 stood out by exhibiting the highest volumetric growth rate, reaching 23.62 m^3 day^{-1} (Table 7). This result reflects substantial expansion in width and, particularly, depth throughout the analyzed period, considering that the removed sediment was effectively transported out of the gully system.

Table 7. Growth rate of the studied erosional incisions (m^3/day).

Gullies.	Volume (m^3) 2017 (A)	Volume (m^3) 2020 (B)	Difference (B – A = C) (m^3)	Cumulative precipitation 2017–2020 (mm)	Volumetric growth rate (m^3 day^{-1}) Total period (850 days)*	Volumetric growth rate (m^3 day^{-1}) Rainfall days only (453 days)**
1	36960,60	39596,77	2636,16	5839,1	3,10	5,81
2	40921,95	51622,89	10700,94	5839,1	12,58	23,62
3	108322,39	92713,75	-15608,65	5839,1	***	***
4	49833,64	19536,60	-30297,04	5839,1	***	***

* Total monitoring period between September 10, 2017 and January 7, 2020.** Days with recorded precipitation during the monitoring period.

*** Growth rate not calculated due to volumetric reduction between monitoring periods. Source: Authors (2026).

5. Discussion

5.1. Morphometric evolution of gullies

As previously discussed, secondary erosional features, such as vertical and subvertical rills, grooves, and other reworking structures, occur along gully margins and contribute to the enlargement of these erosional landforms.

Secondary erosional and reworking features were identified in all four monitored incisions, indicating the continuous activity of erosional processes within the gullies and contributing to their morphological evolution (Oliveira, 1999; Vieira et al., 2011; Guerra et al., 2017; Frota Filho et al., 2020). These features are associated with specific geomorphic mechanisms, and their characteristic morphology reflects the dominant erosional dynamics.

In addition to indicating that the gullies remain active, these structures promote their expansion. Among the main features observed were headcut alcoves, potholes, ribs, pedestals (*demoiselles*), and exfoliation structures.

Tension cracks were observed along the margins and headcut of Gully 01, indicating terrain instability and lateral wall retreat through collapse processes (Figure 14). These features demonstrate that the gully remains active and indicate the occurrence of generalized mass movements contributing to its ongoing evolution. The same growth pattern was identified in the other monitored incisions, following dynamics similar to those described in previous studies (Augustin and Aranha, 2006; Silva et al., 2017; Rocha et al., 2018; Pinto and Araújo, 2020; Xavier et al., 2023).

Based on the presented data, longitudinal growth was consistently lower than transverse expansion. This behavior results from the reduction in the contributing area, corresponding to the stormwater catchment zone, which directly influences the volume of flow directed toward the headcut. In other words, longitudinal growth depends primarily on concentrated surface runoff, whereas transverse expansion is more directly associated with localized erosional processes represented by headcut alcoves, flutings, and torrential potholes that continue to develop within the incisions, as described by Oliveira (1999), Frota Filho et al. (2020), and Vieira and Frota Filho (2023).

Therefore, the reduction in the direct stormwater catchment area caused by incision progression affects the rate of upstream expansion. This behavior is associated with a positive feedback mechanism between flow generation and erosion. Such dynamics occur mainly in disconnected and integrated gullies, according to the typological classification proposed by Oliveira (1989).

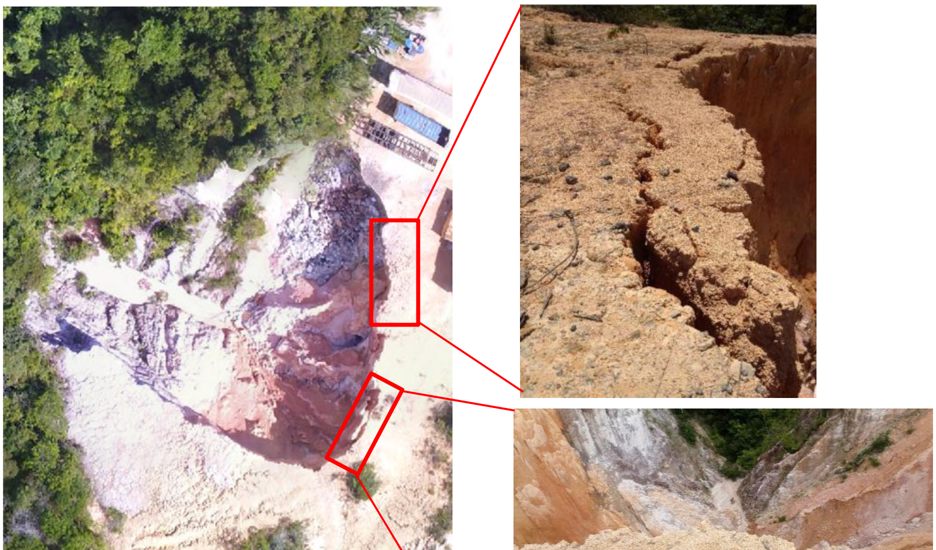

Figure 14. Rills along the margin of Gully 01, Distrito Industrial II neighborhood. Source and prepared by the authors (2026).

Incisions 04 and 05 (Figure 10), developed on the same hillslope and already reaching the summit, were classified as integrated gullies and exhibited progressive widening and coalescence resulting from the collapse of the wall separating them, leading to the formation of a single gully (Figure 15), currently designated as Incision 04. A similar dynamic is likely to occur between Incisions 03 and 04, considering that both exhibited width expansion and increasingly rounded headcuts, progressively approaching a rectangular morphology.

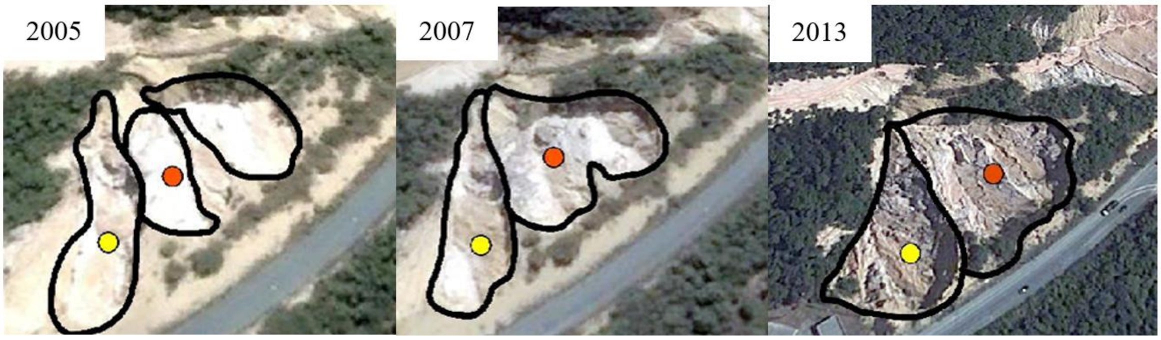

Figure 15. Evolution of gullies in the Distrito Industrial II neighborhood within the Colônia Antônio Aleixo watershed. The yellow marker indicates Gully 03, whereas the orange marker indicates Gully 04. Source: © Google Earth imagery from 2005, 2007, and 2013; prepared by the authors (2026).

Understanding gully morphometry makes it possible to assess the impacts caused by these incisions from both environmental and urban planning perspectives. In the first case, the main impacts include land loss and the volume of sediment transported to drainage channels, promoting channel siltation. This process is further compounded by vegetation mortality resulting from ecological changes caused by sediment accumulation. From an urban planning perspective, the continuous advance of these incisions toward access roads causes pavement damage and deterioration of stormwater drainage infrastructure, among other impacts.

In general, the analyzed gullies exhibit similar characteristics, particularly regarding morphology and hillslope position, especially when associated with anthropogenic forcing as the triggering factor for their development. To a large extent, this process is related to artificial drainage systems composed of channels and stormwater galleries, which convey concentrated water flows capable of intensifying erosional processes and controlling both their direction and expansion.

Upstream of their headcuts, these gullies are bordered by paved roads that accumulate rainfall runoff. This water is captured by drainage systems and subsequently directed into the gullies, promoting their evolution. In this context, Tucci and Collischonn (2000) and Rossato and Botelho (2002) reported that increases in surface paving coefficients intensify urban erosion by approximately 60% to 80%. Consequently, as the proportion of paved streets increases, infiltration areas decrease and surface runoff intensifies, enhancing erosional processes. When these concentrated flows reach exposed soil, their erosive potential increases further. This scenario favors the development of erosional features such as gullies, accelerating their growth and increasing their dimensions, particularly under conditions of intense and concentrated rainfall associated with stormwater channelization.

The erosional dynamics intensified by drainage channels responsible for concentrating stormwater runoff may initiate or enlarge gullies, especially in areas of exposed soil. In the Colônia Antônio Aleixo watershed, the monitored gullies follow the direction of these drainage channels, reflecting a process identified in other studies conducted in urban and roadside environments (Tucci and Collischonn, 2000; Rossato and Botelho, 2002; Jungerius et al., 2002; Valentin and Poesen, 2005; Ferreira et al., 2011; Dirane, 2016, 2018; Frota Filho, 2016, 2021; Silva, 2017, 2020; Silva and Vieira, 2021; Vieira et al., 2022; Guerra et al., 2023; Kuhn et al., 2023). The increase in concentrated runoff associated with artificial drainage systems promotes the development of these erosional landforms.

5.2. Soil Loss Rates and Impacts on the Drainage Network

Regarding the four monitored incisions, including two connected and two integrated gullies, the sediment volumes mobilized by erosion were transported into the fluvial drainage network, which is currently heavily silted. Connected and integrated gullies directly affect fluvial channels, as reported for other sectors of the Colônia Antônio Aleixo watershed (Barbosa, 2013; Frota Filho, 2016, 2021).

To quantify the sediment volume mobilized by the four monitored incisions, the eroded areas were multiplied by the maximum measured depth, yielding the maximum eroded volume for each incision up to the 2020 monitoring survey. To complement this calculation, the mean soil bulk density at the sites where these features developed was applied, enabling the estimation of eroded mass in tons for each incision (Table 8). Conceptually, soil bulk density encompasses the solid, liquid, and gaseous phases, as described by Lepsch (2011).

Table 8. Area, volume, and estimated eroded mass of the monitored gullies.

Gully	Maximum eroded area (m²)	Maximum measured depth (m)	Maximum eroded volume (m³)	Soil bulk density (g cm⁻³)	Eroded mass (t)
1	1 809,06	21,92	39 654,59	1,41	55 912,97
2	1 926,87	26,79	51 620,84	1,41	72 785,38
3	3 483,38	34,69	120 838,45	1,19	143 797,75
4	1 519,32	32,80	49 833,69	1,19	59 302,09
Total	8 738,63	-	261 947,57	-	331 798,19

Source: Authors (2026).

In proportional terms, Gullies 01 and 02 contributed greater sediment mass because of the higher bulk density of the transported material, corresponding to 1.41 g cm^{-3}. Gullies 03 and 04 exhibited lower bulk density values, averaging 1.19 g cm^{-3}, although these two incisions contributed greater absolute sediment volumes. Altogether, the analyzed features supplied approximately 261,947.57 m^3, or 331,798.19 t, of sediment to the drainage network (Figure 16), which is currently heavily silted because of the continuous input of sediment from these incisions.

The impacts become more pronounced in connected and integrated gullies because these features are directly linked to the drainage network. Consequently, sediment is delivered directly, with limited potential for retention or deposition along midslope positions or at hillslope toes. In general, Barbosa (2013) indicated that gullies contribute substantial volumes of sediment to the Colônia Antônio Aleixo watershed, with much of this material remaining within the basin, particularly the coarser fraction, represented by sand, whereas the finer fractions, represented by silt and clay, are transported directly to the Amazon River.

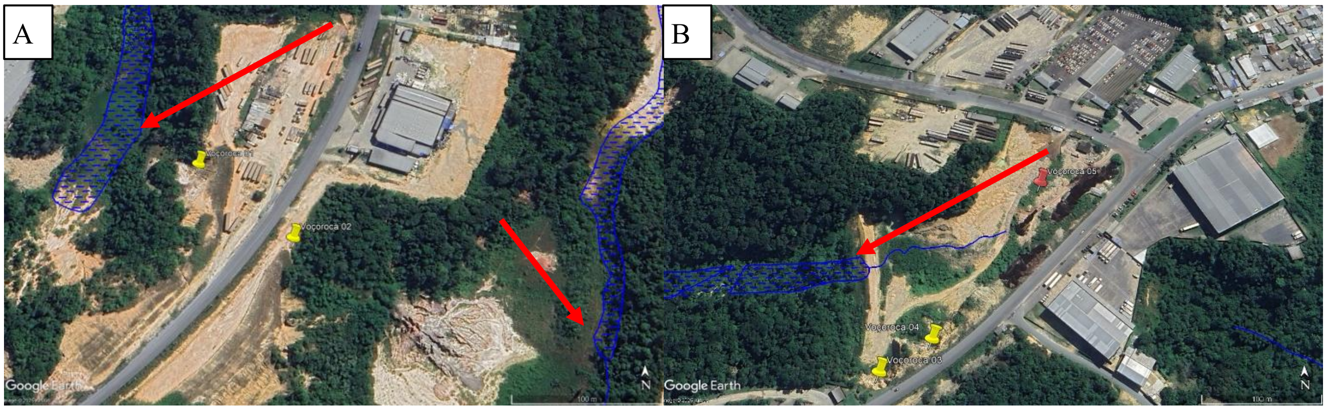

Figure 16. (A) Gullies 01 and 02. (B) Gullies 03, 04, and 05. Partial view of the drainage network silted by sediments derived from the gullies (red arrows) in the Distrito Industrial II neighborhood. Source: Google Earth imagery (2024), scale 1:10,000; prepared by the authors (2026).

Another condition directly associated with siltation in the Colônia Antônio Aleixo watershed is the low discharge of the main channel. Abdon (2004), Camargo (2012), and Mugade and Sapkale (2015) confirmed the relationship between channel discharge and siltation, indicating that this process occurs when sediment deposition rates exceed the channel's transport capacity.

However, finer sediments, represented by the clay and silt fractions, are transported through the channel network and subsequently exported beyond the watershed boundaries. This behavior is corroborated by suspended sediment concentrations observed in the lower third of the main channel, ranging from 2.0 to 2.4 mg L^{-1} (Barbosa, 2013). Sediment deposition and the resulting siltation may induce morphological adjustments in channel geometry and alter interactions between surface and subsurface flows, favoring the expansion of erosional surfaces (Golosov, 2002; Thakur, 2019).

.

6. Conclusions

The application of UAVs has proven to be an efficient alternative for overcoming limitations commonly encountered during field-based diagnosis and monitoring of erosional features. Under conditions of restricted access or elevated physical risk, this remote sensing approach provides a viable and safe solution. Its ability to generate high-spatial-resolution data is particularly suitable for perimeter delineation, area and volume estimation, and the construction of longitudinal and transverse profiles.

In the present study, UAVs were employed to monitor gully evolution and associated secondary features, such as headcut alcoves and rills. The adopted methodology was based on aerial photogrammetric surveys followed by geoprocessing analysis, yielding more precise results than traditional methods such as stake-based surveys and planimetric polygonal measurements. This procedure enabled the monitoring of incision dynamics, the differentiation of developmental stages, and the identification of associated erosional elements, although field verification remains essential for complementary validation.

Digital Elevation Models (DEMs) generated from the acquired imagery were used to calculate the volume of soil eroded throughout the evolutionary process of the analyzed gullies. Data reliability was verified through comparison with topographic profiles collected in the field, showing variations of less than 10%. By relating volumetric estimates to mean soil bulk density, it was possible to estimate the mass of displaced sediment. Across the four monitored gullies, the estimated eroded volume reached 261,947.57 m^3, corresponding to approximately 331,798.19 t of transported material. These values highlight the substantial sediment load mobilized and reinforce the importance of this type of analysis for understanding the impacts of erosion on urban drainage networks.

Secondary erosional features, such as headcut alcoves, were identified within the gullies and were shown to contribute to incision advance. Comparison of topographic profiles, particularly for Gullies 01 and 02, revealed the formation of rills along the margins of the main incision. This behavior indicates active erosional sectors and suggests ongoing lateral expansion. These analyses enabled the estimation of morphometric evolution rates and the identification of preferential erosion directions. Longitudinal and transverse profiles further demonstrated the influence of factors such as stormwater runoff and anthropogenic land-use disturbance. In this context, the direction of gully expansion was shown to be primarily controlled by human interventions.

Systematic and continuous gully monitoring enables the identification of highly vulnerable zones and the mapping of preferential growth directions of erosional features. Such information is particularly relevant in areas adjacent to roads, residences, and urban infrastructure, where geotechnical risk is elevated. In these contexts, UAV-based monitoring offers strong potential for both diagnosis and support for erosion control, containment, and environmental rehabilitation measures.

The results demonstrate that erosional processes in urban areas are directly associated with disordered occupation patterns and inadequate territorial planning. These findings reinforce the need for public policies focused on geotechnical risk management and the incorporation of remote sensing technologies, such as UAVs, into continuous monitoring programs for these vulnerable environments.

Author's contributions: Conceptualization, Frota Filho, A.B., Vieira, A.F.S.G., and Guerra, A.J.T.; methodology, Frota Filho, A.B., Vieira, A.F.S.G., and Guerra, A.J.T.; validation, Frota Filho, A.B. and Vieira, A.F.S.G.; formal analysis, Frota Filho, A.B. and Vieira, A.F.S.G.; investigation, Frota Filho, A.B., Vieira, A.F.S.G., and Guerra, A.J.T.; resources, Frota Filho, A.B., Vieira, A.F.S.G., and Guerra, A.J.T.; data curation, Frota Filho, A.B.; writing—original draft preparation, Frota Filho, A.B. and Guerra, A.J.T.; writing—review and editing, Frota Filho, A.B. and Vieira, A.F.S.G.; supervision, Vieira, A.F.S.G. and Guerra, A.J.T.; project administration, Frota Filho, A.B., Vieira, A.F.S.G., and Guerra, A.J.T.; funding acquisition, Vieira, A.F.S.G. All authors have read and agreed to the published version of the manuscript.

Acknowledgements: The authors gratefully acknowledge the financial support provided by CAPES and FAPEAM for the development of this research. The doctoral research of the first author, which provided the foundation for this study, was funded through scholarships granted by CAPES and CNPq. The second and third authors also acknowledge the Brazilian National Council for Scientific and Technological Development (CNPq) for the productivity research fellowships granted.

Statement on the Use of Artificial Intelligence: The authors used the artificial intelligence tool ChatGPT (OpenAI) to assist with the grammatical revision of the manuscript in Portuguese, the translation of selected passages into English, and the visual enhancement of Figure 4. The use of this tool was limited to linguistic improvement and textual refinement and was not employed in the design of the study, data collection, data analysis, interpretation of results, or formulation of the study's conclusions. The authors thoroughly reviewed and validated all AI-generated content and assume full responsibility for the final version of the manuscript.

Conflict of Interest: The authors declare no conflict of interest.

References

1. AUGUSTIN, C.H.R.R.; ARANHA, P.R.A. Piping em área de voçorocamento, noroeste de Minas Gerais. Revista Brasileira de Geomorfologia. Ano 7, nº 1, p. 09-18, 2006.DOI: https://doi.org/10.20502/rbg.v7i1.56
2. BARBOSA, A.J. Voçorocas e a produção de sedimentos na bacia da Colônia Antônio Aleixo em Manaus (AM). 2013, 81 f. Dissertação (Mestrado em Geografia), Programa de Pós-graduação em Geografia. Universidade Federal do Amazonas, Manaus, 2013.
3. BITENCOURT, C.; FERNANDES, C. A.; RODRIGUES, E. C.; TEIXEIRA, M. A. Aplicações da técnica SfM-MVS em mapeamentos geomorfológicos com uso de VANT: estudo de caso em área urbana no Rio Grande do Sul. Geociências (São Paulo), v. 40, n. 1, p. 195–210, 2021. Disponível em: https://www.scielo.br/j/gcg/a/CrnhLgNhQCTzSvZTtcxdxbg. Acesso em: 12 maio 2025.
4. BORRELLI, P., BALLABIO, C., YANG, JE., ROBINSON, DA. & PANAGOS, P. GloSEM: High-resolution global estimates of present and future soil displacement in croplands by water erosion, figshare, https://doi.org/10.6084/m9.figshare.c.5844758.v1 (2022).
5. CROZIER, M. J.; Hardenbicker, U.; GOMEZ, B. Physical Landscapes In: GOMEZ, B.; JONES, J.P. Research Methods in Geography. Oxford: Blackwell Publishing., 2010, 459 p.
6. D´ÁVILA JUNIOR, J.C.M.; VIEIRA, A.F.S.G. Padrões pluviométricos da cidade de Manaus-AM: 1986 a 2015. In: Boletim Paulista de Geografia. n.102, dez. 2019. p.1-31
7. DIRANE, A.C.M. Mapeamento das áreas de risco a voçorocamento e caracterização geoambiental da rodovia AM-010 Manaus/Itacoatiara – AM. 2016. 106f. Dissertação (Mestrado em Geografia). Programa de Pós-graduação em Geografia. Universidade Federal do Amazonas. Manaus. 2016.
8. FERREIRA, V.M.; SILVA, M.L.N.; CURI, N.; OLIVEIRA, A.H.; SILVA, M.A.; AVANZI, J. C. Influência antrópica e atributos de solo: inter-relações em ambientes de voçorocas na mesorregião Campos das Vertentes, MG. Geografia, Rio Claro, v. 36, p. 209-219, 2011
9. FRANZINELLI, E. e PIUCCI, J. (1988). Evidências de neotectonismo na Bacia Amazônica. In: VII Congresso Latino-Americano de Geologia. Anais [...]. Belém. p. 80-90.
10. FROTA FILHO, A.B. Análise da vulnerabilidade erosiva da bacia hidrográfica colônia Antônio Aleixo, Manaus-AM. 2016. Dissertação (Mestrado em Geografia). Programa de Pós-Graduação em Geografia, UFAM, Manaus. 2016.
11. FROTA FILHO, A.B. Alterações antropogênicas na geomorfologia e suas influências na aceleração dos processos erosivos, bacia hidrográfica colônia Antônio Aleixo, Manaus-Am. 2021. 258f. Tese (Doutorado em Planejamento e Gestão Ambiental) - Instituto de Geociências – IGEO, Universidade Federal do Rio de Janeiro, Rio de Janeiro, 2021.
12. FROTA FILHO, A.B.; ABREU, N.R.P.; VIEIRA, A.F.S.G. Processo de voçorocamento e feições secundárias: um estudo de caso em Manaus-AM. Revista Caminhos de Geografia, v. 21, p. 313-323, 2020. Disponível em: doi.org/10.14393/RCG217441778. https://seer.ufu.br/index.php/caminhosdegeografia/article/view/41778. Acesso em: 14/01/2024
13. GOLOSOV, V. Soil erosion and small river aggradation in Russia. In: ISCO Conference. 12., 2002.Beijing. Proceedings […]. Beijing: 2002. p. 154-159.
14. GUERRA, A.J.T. e GUERRA, A. J. T. Novo Dicionário Geológico -Geomorfológico. 3 ed. Rio de Janeiro: Bertrand Brasil, 2004. 652p.
15. GUERRA, ANTÔNIO JOSÉ TEIXEIRA; FULLEN, MICHAEL AUGUSTINE ; JORGE, MARIA DO CARMO OLIVEIRA ; Bezerra, José Fernando Rodrigues ; SHOKR, MOHAMED . Slope Processes, Mass Movement and Soil Erosion: A Review. Pedosphere, v. 27, p. 27-41, 2017.
16. GUERRA, A. J. T.; BEZERRA, J. F. R. ; JORGE, M. C. O. Recuperação de voçorocas e de áreas degradadas, no Brasil e no mundo – estudo de caso da voçoroca do Sacavém – São Luís – MA, 2023.
17. JUNGERIUS, P.D.; MATUNDURA, J.; VAN DE ANCKER, J.A.M. Road construction and gully erosion in West Pokot, Kenya. Earth Surface Processes and Landforms, 27(11), 1237–1247. 2002. doi:10.1002/esp.423
18. KRENZ, J.; GREENWOOD, P.; HECKRATH, G.; KUHN, B.; KUHN, N. Assessing Badland Sediment Sources using UAVs. In: EGU General Assembly Conference Abstracts. 2018. p. 8126.
19. KRENZ, J.; GREENWOOD, P.; KUHN, N. J. Soil Degradation Mapping in Drylands Using Unmanned Aerial Vehicle (UAV) Data. Soil Systems, 3(2), 33. 2019. doi:10.3390/soilsystems3020033
20. KRENZ, J.; KUHN, N.J. Assessing Badland Sediment Sources Using Unmanned Aerial Vehicles. Badlands Dynamics in a Context of Global Change, 2018. 255–276. doi:10.1016/b978-0-12-813054-4.00008-3

21. KUHN, C.E.S.; REIS, F.A.G.V.; ZARFL, C.; GRATHWOHL, P. Ravines and gullies, a review about impact valuation. Natural Hazards, 117(1), 597-624. 2023.
22. LEAL, P.C. Caracterização e interpretações genéticas de alguns solos da região de Manaus-AM. 1996. 109f. Dissertação (Mestrado). Programa de Pós-graduação em Ciência dos Solos. Universidade Federal Rural de Pernambuco. Recife, 1996.
23. LEPSCH, I. F. 19 lições de pedologia. São Paulo: Oficina de Textos, 2011, p. 793.
24. LOUREIRO, H. A. S.; GUERRA, A. J. T.; ANDRADE, A. G. Contribuição ao estudo de voçorocas a partir do uso experimental de laser scanner terrestre e VANT. Revista Brasileira de Geomorfologia, v. 21, n. 4, 871-892, 2020
25. LOUREIRO, H.A.S. Diagnóstico de erosão por voçorocas: experimentos com geotecnologias e solos na bacia do Alto rio Piraí - Rio Claro-RJ. 2019. 224 f. Tese (Doutorado em Geografia – Planejamento e Gestão Ambiental) – Programa de Pós-graduação em Geografia, Instituto de Geociências, Universidade Federal do Rio de Janeiro, Rio de Janeiro, 2019.
26. OLIVEIRA, M.A.T. Erosion Disconformities and Gully Morphology: A Threedimensional Approach. In: Catena: na interdisciplinary journal of Soil Science Hydrology – Geomorphology. Vol. 16. W. Germany: Catena Verlag. 1989. p. 413-423
27. OLIVEIRA, M.A.T. Processos erosivos e preservação de áreas de risco de erosão por voçorocas. In: Guerra, A.J.T.; Silva, A.S.; Botelho, R.G.M. (Org). Erosão e Conservação dos solos: conceitos, temas e aplicações. 1. ed. Rio de Janeiro: Bertrand Brasil, 1999. p 57-99.
28. OLIVEIRA, M.A.T.; LEMOS, R.; PINTO, L.R. Pode uma voçoroca resultar da evolução de voçorocas conectadas e desconectadas?. Revista Brasileira de Geomorfologia, [S. l.], v. 24, n. 00, 2023. DOI: 10.20502/rbg.v24i00.2372. Disponível em: https://www.rbgeomorfologia.org.br/rbg/article/view/2372. Acesso em: 15 jan. 2024.
29. PINTO, B.L.; ARAÚJO, H.M. Configuração geomorfológica contemporânea de uma voçoroca sobre a litoestrutura sedimentar da sub-bacia de tucano central–BA. Acta Geográfica, v. 14, n. 35, p. 1-26, 2020.
30. ROCHA, W.S.; PASQUALETTO, A.; SANTOS, G.M.; MENDES, T.A.; SANTOS, H.I. Erosão Urbana: Microbacia do Córrego Olho D'água, Município de Goiânia, Goiás. Revista Baru-Revista Brasileira de Assuntos Regionais e Urbanos, 4(1), 64-76. 2018.
31. ROSSATO, M. S.; BOTELHO, R. G. M. Erosão urbana no brasil. Revista Da Pós-Graduação em Geografia, Rio de Janeiro, v. 5, p. 33-52, 2002.
32. ROSS, J.LS. Fundamentos da Geografia da Natureza. In: ROSS. J.L.S. (org.). Geografia do Brasil. São Paulo: EDUSP, 2000. p.13-65
33. SANTANA, G.F. Análise dos padrões térmicos da cidade de Manaus-AM no período de 1986 a 2015. 2018. 47f. Relatório de Pesquisa. Pró-reitoria de Pesquisa e Pós-graduação. Universidade Federal do Amazonas. Manaus, 2018.
34. SANTANA, G.F. Monitoramento de voçorocas utilizando veículo aéreo não tripulado (VANT) em áreas de difícil acesso em Manaus-AM. 2019. 31f. Relatório de Pesquisa. Pró-reitoria de Pesquisa e Pós-graduação. Universidade Federal do Amazonas. Manaus, 2018.
35. SILVA, D.G.; CÔRREA, A.C.B.; AMORIM, R.F. Caracterização morfológica e dinâmica ambiental das marmitas (weathering pit) no distrito de Fazenda Nova, Pernambuco – Nordeste do Brasil. Revista Brasileira de Geomorfologia, [S.l.], v.18, n.2, 2017. DOI: 10.20502/rbg.v18i2.1062. Disponível em: https://rbgeomorfologia.org.br/rbg/article/view/1062. Acesso em: 7 nov. 2023.
36. SILVA, G.M. Geomorfologia aplicada à caracterização da vulnerabilidade à erosão em Rio Preto da Eva (AM). 2021. 113f. Dissertação (Mestrado em Geografia). Programa de Pós-graduação em Geografia. Universidade Federal do Amazonas. Manaus. 2021.
37. SILVA, G.M.; VIEIRA, A.F.S.G. Mapeamento de voçorocas na cidade de Rio Preto da Eva (AM). Geosaberes: Revista de Estudos Geoeducacionais, v. 11, 2020. p. 517-531.
38. SILVA, G.M.; VIEIRA, A.F.S.G.; ALVES, A.S. Análise da ocupação da terra em área de risco: um estudo de caso no Bairro Nova Cidade, Manaus-AM. Caderno de Geografia. v.33, n.7, 2023. p.93-109
39. SILVA, I.N. Geomorfologia e planejamento ambiental: identificação e monitoramento de voçorocas no sítio urbano de Iranduba/AM. 2020. 166f. Dissertação (Mestrado em Geografia). Programa de Pós-graduação em Geografia. Universidade Federal do Amazonas. Manaus. 2020.
40. SILVA, I.N.; VIEIRA, A.F.S.G. Mapeamento de voçoroca no sítio urbano de Iranduba – AM. In: VIEIRA, A.F.S.G.; MOLINARI, D.C. (Orgs.). Geografia Física da Amazônia - Volume 2. São Paulo/Manaus: Alexa Cultural/EDUA, 2021. p.71-88
41. SOUSA, K.C.D Avaliação geométrica de imagens adquiridas por Veículo Aéreo Não Tripulado (VANT) para o mapeamento de feições erosivas em Manaus-AM. Relatório de Iniciação Científica – Universidade Federal do Amazonas, 2018.

42. SPELL, R.L.; JOHNSON, B.G. Anthropogenic alluvial sediments in North Carolina Piedmont gullies indicate swift geomorphic response to 18th century land-use practices. Physical Geography, 1–17. 2019. doi:10.1080/02723646.2019.1574145
43. THAKUR, V. K. Sediment management of Nathpa dam from heavy silt in river Satluj (India) preparing a one column paper with word for windows. In: TOURNIER, J. P.; BENNETT, T.; BIBEAU, J. Sustainable and safe dams around the world. CRC Press, 2019. p. 1327-1337.
44. VALENTIN, C.; POESEN, J.; LI, Y. Gully erosion: Impacts, factors and control. Catena, v. 63, n. 2-3, p. 132-153, 2005.
45. VIEIRA, A.F.G. Desenvolvimento e distribuição de voçorocas em Manaus (AM): principais fatores controladores e impacto urbano ambientais. 2008. 310f. Tese (Doutorado em Geografia). Programa de Pós-graduação em Geografia. Universidade Federal de Santa Catarina. Florianópolis. 2008.
46. VIEIRA, A.F.G. Erosão por voçorocas em áreas urbanas: o caso de Manaus (AM). 1998. 181f. Dissertação (Mestrado em Geografia). Programa de Pós-graduação em Geografia. Universidade Federal de Santa Catarina. Florianópolis. 1998.
47. VIEIRA, A.F.G.; ALBUQUERQUE, A.R.C. Cadastramento de voçorocas e análise de risco erosivo em estradas: BR-174 (Trecho Manaus – Presidente Figueiredo). In: V Simpósio Nacional de Geomorfologia e I Encontro Sul-Americano de Geomorfologia (SINAGEO/ESG), 5., 2004, Santa Maria. Anais... Santa Maria: UGB/UFSM, 2004. p. 50-65
48. VIEIRA, A.F.G.; MOLINARI, D.C.; DIRANE, A.C.M.; DONALD, A.R. Condicionantes morfométricos para o surgimento de caneluras e escamamentos em voçorocas. Revista Geonorte, v. 01, p. 79-92, 2011.
49. VIEIRA, A.F.S.G.; LIMA, C.M.R.; SILVA, G.M. Caracterização das voçorocas da área urbana de Rio Preto da Eva (AM), Norte do Brasil. Geologia USP, Série Científica, São Paulo, v. 22, n. 4, 2022. p. 9-107
50. VIEIRA, A.F.S.G.; FROTA FILHO, A.B. Avaliação das técnicas de monitoramento de voçorocas: o exemplo da Região Metropolitana de Manaus-AM, na região amazônica. Revista Brasileira De Geomorfologia, v.24, n. Especial, 2023. Disponível em: https://doi.org/10.20502/rbg.v24i00.2302 Acesso em 15/01/2024
51. WELDEYOHANIS, Y.H.; ANESEYEE, A.B.; SODANGO, T.H. Evaluation of current solid waste disposal site based on socio-economic and geospatial data: a case study of Wolkite town, Ethiopia. GeoJournal, 87(2), 585-601. 2022.
52. XAVIER, R.A.; BORGES NETO, I.O.; SOUZA, J.J.L.L.; CARDOSO, P.V.; SOUZA, J.O.P.; SOUZA, B.I. Processos de voçorocamento no Planalto da Borborema, semiárido da Paraíba. Revista Brasileira de Geomorfologia, [S. l.], v. 24, n. 00, 2023. DOI: 10.20502/rbg.v24i00.2359. Disponível em: https://rbgeomorfologia.org.br/rbg/article/view/2359. Acesso em: 07/11/2023.
53. XU, Q.; KOU, P.; WANG, C.; YUNUS, A.P.; XU, J.; PENG, S.; HE, C. Evaluation of gully head retreat and fill rates based on high-resolution satellite images in the loess region of China. Environmental Earth Sciences, 78(15). 2019. doi:10.1007/s12665-019-8483-x
54. ZOLEZZI, G.; BEZZI, M. Urban gully erosion and the SDGs: a case study from the Koboko rural town of Uganda. In: EGU General Assembly Conference Abstracts. 2017. p. 11687.